Received: 23 January 2021 | Revised: 21 March 2021 | Accepted: 6 April 2021

DOI: 10.1002/ar.24649

FULL LENGTH ARTICLE

The Anatomical Record

WILEY

Microvascular anatomy of the non-lobulated liver of adult *Xenopus laevis*: A scanning electron microscopic study of vascular casts

Alois Lametschwandtner[1] | **Udo Spornitz**[2] | **Bernd Minnich**[1]

[1]Department of Biosciences, University of Salzburg, Vascular and Exercise Biology Research Group, Salzburg, Austria

[2]Department of Biomedicine, University of Basel, Basel, Switzerland

Correspondence
Alois Lametschwandtner, Department of Biosciences, University of Salzburg, Vascular and Exercise Biology Research Group, Hellbrunnerstrasse 34, A-5020 Salzburg, Austria.
Email: alois.lametschwandtner@sbg.ac.at

Funding information
Universität Salzburg

Abstract

The microvascular anatomy of the non-lobulated liver of adult *Xenopus laevis* was studied by scanning electron microscopy of vascular corrosion casts. Hepatic portal veins and hepatic arteries entered hepatic lobes at the hiluses, hepatic veins left at these sites. Intraparenchymal, hepatic portal veins branched up to 10 times before terminal portal venules supplied liver sinusoids. Hepatic arteries closely followed portal vessels. Arteriolar side branches formed anastomoses with close by portal venules (arteriolar-portal anastomoses; APAs), liver sinusoids (arteriolar-sinusoidal anastomoses; ASAs), and peribiliary plexus vessels. Distally, hepatic arteries anastomosed with terminal portal venules having >100 μm in diameter. Liver sinusoids formed a dense three-dimensional network displaying signs of non-sprouting and sprouting angiogenesis evidenced by "holes" and blind ending tapering cast vascular structures (sprouts), respectively. Sinusoids drained via efferent hepatic veins. Right and left hepatic veins drained into the posterior caval vein. Locally, a dense honeycomb-like 3D-meshwork of resin structures was found around terminal portal venules and hepatic arteries. These networks were fed by hepatic arterioles and drained into adjacent terminal portal venules. As their morphologies differed significantly from sinusoids and they were found at sites where diffuse lymphoid tissue is described, we are convinced that they represent the vasculature of diffuse lymphoid tissue areas. Frequencies and diameter ratios of hepatic portal venules versus hepatic arterioles anastomosing with the former (APAs) implicate that the arterial supply contributes to the oxygenation of parenchymal and stromal cells rather than to a significant increase in blood flow towards hepatic sinusoids.

Abbreviations: at, arterial trunk; av, abdominal vein; bd, bile duct; ebdv, efferent bile duct venule; ehv, efferent hepatic vein/venule; gb, gallbladder; ha, hepatic artery/arteriole; hv, hepatic vein/venule; l, lateral; lhv, left hepatic vein; li, large intestine; ll, left lobe; ltv, lymphoid tissue vasculature; m, medial; p, posterior; pa, pulmonary artery; pcv, posterior caval vein; pv, portal vein; rhv, right hepatic vein; rl, right lobe; s, sinusoid; sa, systemic arch; SEM, Scanning Electron Microscopy; si, small intestine; tpv, terminal portal vein/venule; VCC, Vascular Corrosion Cast; vv, venule.

KEYWORDS
liver, microvasculature, scanning electron microscopy, vascular casts, *Xenopus*

1 | INTRODUCTION

Liver structure and function in health and disease are best studied in mammals and humans whereby many studies were devoted to hepatic circulation (Geerts, Timmermans, & Reynaert, 2008; McCuskey, 2000, 2008; Sasse, Spornitz, & Maly, 1992). Presently, hepatic microvascular anatomy is convincingly illustrated by vascular corrosion casts examined either by scanning electron microscopy (SEM) (McCuskey, 2008; Murakami, 1971; Murakami, Itoshima, & Shimada, 1974; Ohtani, 1981a, 1981b, 1989; Ohtani, Kikuta, Ohtsuka, Taguchi, & Murakami, 1983; Ohtani & Murakami, 1978; Ohtani, Murakami, & Jones, 1982; Yamamoto, Sherman, Phillips, & Fisher, 1985) or by high resolution computer-tomography (CT) (Chen, Yue, Zhong, & Wang, 2016; Debbaut et al., 2014; Fasel, 2008; Peeters et al., 2017).

We have a comprehensive knowledge on liver microvascular anatomy and hepatic circulation in mammals and humans. In the African clawed toad, *Xenopus laevis*, which has become a model organism to gain insights into fundamental processes in embryology, cell biology, genetics, physiology, toxicology, evolution, ecology, and disease (Griffin, Liu, & Sempou, 2020), we still lack this knowledge. We know *Xenopus* liver anatomy (Porro & Richards, 2017; Storch & Welsch, 1996), histology (Akiyoshi & Inoue, 2012; Wiechmann & Wiechmann-Wirsig, 2003), ultrastructure (Spornitz, 1975a, 1975b), and gross blood supply and drainage routes (Millard, 1940). We also have first insights into its microvascular architecture (Häring, 2004), but an in-depth analysis of the latter is still lacking.

We used SEM of vascular corrosion casts (Aharinejad & Lametschwandtner, 1992; Lametschwandtner, Lametschwandtner, & Weiger, 1990; Motta, Murakami, & Fujita, 1992; Murakami, 1971) and analyzed the microvascular anatomy of the non-lobulated liver in the adult *Xenopus*. The high depth of focus and the sufficiently good resolution gained in the conventional scanning electron microscope operated at an acceleration voltage of 10 kV allowed to identify cast capillaries as the blood vessels with the thinnest (luminal) diameter and to differentiate arteries and veins by their characteristic endothelial cell nuclei imprint patterns displayed on the surface of vascular casts (Miodonski, Hodde, & Bakker, 1976). In detail, we elucidated intrahepatic courses and branching patterns of the hepatic portal vein, followed transitions of terminal portal venules into sinusoids and sinusoidal outlets into the hepatic venous system. We highlighted course and targets of supply of the hepatic artery and its branches, and documented the course of efferent hepatic venules and veins. Finally, we looked for blood flow regulating structures like arterial and venous sphincters (Aharinejad, Böck, Lametschwandtner, Franz, & Firbas, 1991; Franz, Böck, Lametschwandtner, Breiteneder, & Firbas, 1990; Schraufnagel & Patel, 1990), flow dividers and intimal cushions (Bond, Chih-Wen, Hanjoong, & Weinberg, 2010; Casellas, Dupont, Jover, & Mimran, 1982; Fourman & Moffat, 1961). The study aimed to figure out which vascular structures *X. laevis* shares with mammalian and human livers and which ones differ from them.

2 | MATERIALS AND METHODS

2.1 | Animals

Thirteen adult animals (6 females, 7 males; body weights: 19 g to 79 g; body lengths: 60 mm to 85 mm) of the African Clawed Toad, *X. laevis* (Daudin, 1802) were studied. Adults were housed in aquaria (tap water depth: 15 cm) equipped with aquarium filters and fed twice a week with either dried *Gammarus pulex* or ground beef heart.

2.2 | Vascular casting

Animals were euthanized by immersion into a 0.5% aqueous solution of MS 222 (Tricaine methansulfonate, Aldrich Chemie, Germany). After measuring body weigths, the heart was exposed, the sinus venosus opened and the circulatory system was rinsed with Amphibian Ringer solution (Adam & Czihak, 1964) via the truncus arteriosus. The flow rate of the infusion pump (Habel, Vienna) was set to 41 mL/h. When clear reflux drained from the opened sinus venosus 10 mL of Mercox CL-2B (Dainippon Ink and Chemicals, Tokyo, Japan; Ladd Burlington, VT) diluted with monomeric methylmethacrylate (4 + 1, v + v, 10 mL monomeric methylacrylate contained 0.85 g initiator paste MA) were injected with the infusor at the same flow rate. When the effluent resin became viscous or the whole amount of resin had been perfused the injection was stopped and the animals were left for about 30 min at room temperature to allow

hardening (polymerization) of the injected resin. After tempering the injected resin by putting the casted animal into a water-bath (60°C; 12–24 hr), specimens were macerated in potassium hydroxide (7.5%; 40°C; 2–24 hr), rinsed three times in distilled water, submerged in 2% hydrochloric acid (1–6 hr), rinsed again three times in distilled water, and submerged in formic acid (5%; 20°C; 5–15 min) to remove residual organic tissues from the cast surfaces. Finally, specimens were rinsed another three times in distilled water and frozen in fresh distilled water. Ice-embedded casts were freeze-dried in a Lyovac GT2 (Leybold-Heraeus, Cologne, Germany). Liver lobes were excised and mounted with either the parieto-pleural or the viscero-pleural surface upside onto specimen stubs using the "conductive bridge-method" (Lametschwandtner, Miodonski, & Simonsberger, 1980) to avoid specimen charging when examined under the SEM. Mounted specimens were either evaporated with carbon and gold (large specimens) or sputter-coated with gold (small specimens) to render the casts conductive when examined under the scanning electron microscope ESEM XL-30 (FEI, Eindhoven, The Netherlands) at an accelerating voltage of 10 kV.

In two specimens, course, branching patterns and areas of supply (or drainage) of individual hepatic vessels were exposed by ripping off overlaying vessels with fine tipped insect pins under binocular control.

Some liver casts were sectioned transversely, some longitudinally or tangentially while embedded in ice. For more details on cutting ice-embedded vascular casts we refer to Lametschwandtner and Lametschwandtner (1992).

To gain first qualitative insights into the ratios of diameters of hepatic portal veins and venules and of flanking hepatic arteries and arterioles we made linear measurements from 2D-scanning electron microscopic images. Data given are not corrected for errors resulting from 2D measurements and shrinkage of the casting medium and thus underestimate linear distances (for details on 2D vs. 3D measurements see Minnich & Lametschwandtner, 2000; for shrinkage data of casting media see Weiger, Lametschwandtner, & Stockmayer, 1986).

To enable less experienced readers to easily distinguish arteries from veins in SEM micrographs we identified casts of arteries and veins by their characteristic surface endothelial cell nuclei imprints (Miodonski et al., 1976) and color-coded hepatic arteries in red, hepatic portal veins in blue and hepatic veins in blue-green by Photoshop 7.0 (Adobe Inc., Redwood, CA).

3 | RESULTS

The liver of *X. laevis* consisted of a left, a right and a very small middle lobe. Right and left lobes differed in size with the left one being the larger one (Figure 1-1). The liver showed a double blood supply via the hepatic portal vein and the hepatic artery (Figure 1-2). It drained via the hepatic vein into the posterior caval vein. Hepatic vessels arrived at the liver hilus, which is located at the ventral (viscero-pleural) surface of right and left liver lobes close to their cranio-medial margins (Figure 1-2). Average vessel (luminal) diameters were: hepatic portal vein: 0.8 mm – 1.14 mm; hepatic artery: 0.38 mm – 0.46 mm; hepatic vein: 1.7 mm – 2.2 mm.

In most specimens, a single hepatic portal vein branched extraparenchymally into a right and a left branch, feeding the right, and left lobe of the liver. In one animal, separate portal veins derived from the ascending and the transverse portions of the distal small intestine and supplied the right and left lobe of the liver individually. In this case, the abdominal vein drained into the left portal vein. An anastomosis connected with the right portal vein.

Generally, the hepatic portal vein branched at the viscero-pleural surface into several first order branches (Figure 1-2). These branches ran superficially over varying distances before they entered the liver parenchyma and became covered by the most superficial sinusoids (Figure 1-2). In two animals, the hepatic portal vein entered the parenchyma immediately at the hilus with no conspicuous superficial branching. Locally, casted branches of the portal vein revealed slender longish imprints of endothelial cell nuclei which were orientated parallel to the longitudinal axis of the vein.

Intraparenchymal, portal veins repeatedly branched in a tree-like pattern and finally formed terminal portal venules of different lengths and diameters (Figures 1-3, 2, 3). Branching modes ranged from simple bifurcations with branching angles from acute to obtuse and to spruce tree-like branchings with several branches of almost the same diameters branching off at the same level (Figure 4-1). Portal vessels could be easily identified by their accompanying hepatic arteries (Figures 1-3, 2, 3). Terminal portal venules extended to the pleural surfaces, where they supplied sinusoids (Figure 4-2). They either remained below the sinusoids or ran over some distance superficially (Figure 4-2). Their nature as terminal portal venules was disclosed by tracing them downstream towards their identifiable mother vessel by microdissection. In central areas, small terminal portal venules originated even from large caliber portal venules (Figure 2) where they often revealed narrowings.

At their transition sites (inlet portions) into hepatic sinusoids, terminal portal venules revealed diameters in the range of 22–29 μm. In many cases, these inlet portions displayed a tube-like morphology. Sinusoids displayed outbulgings and narrowings and also

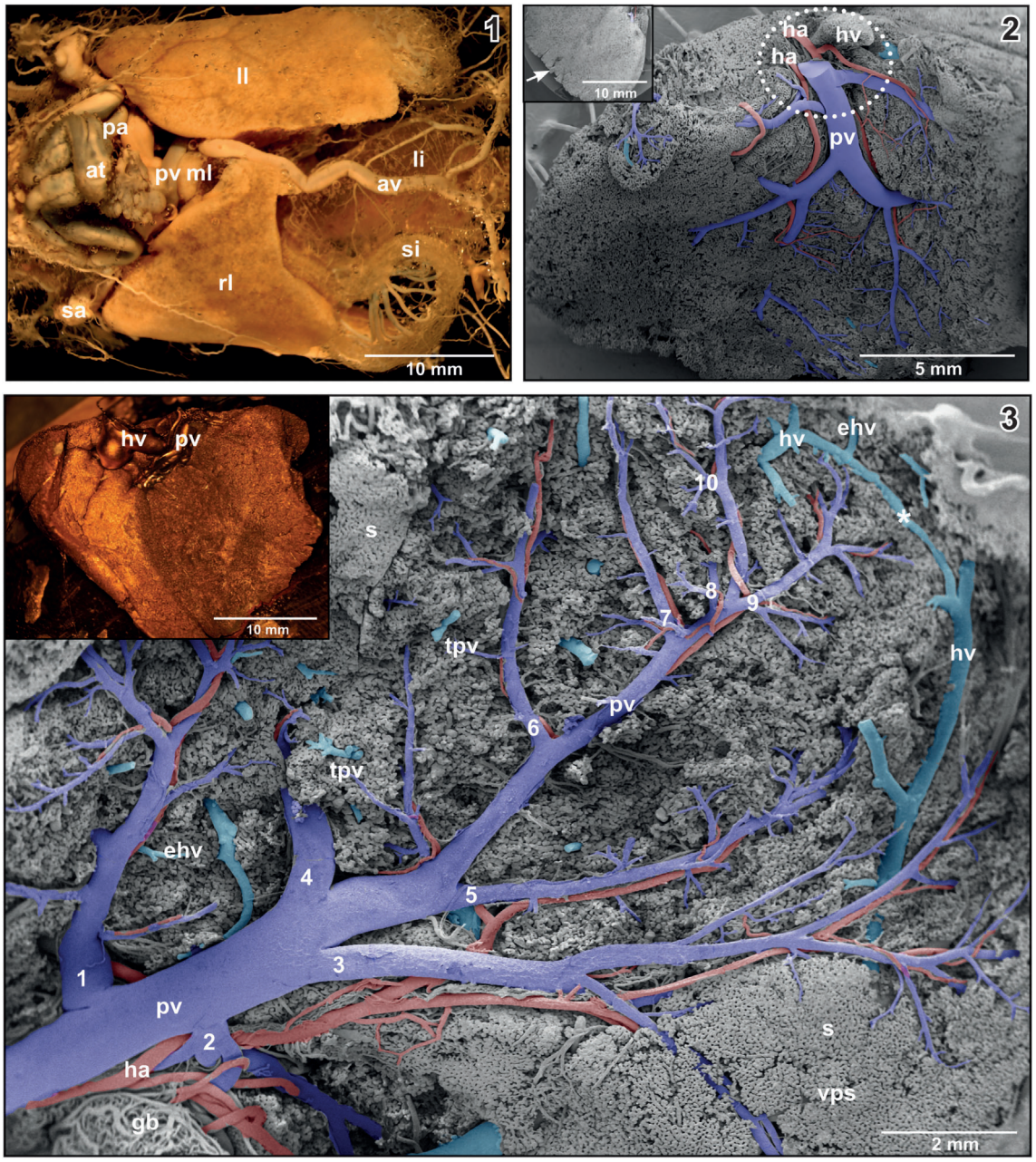

FIGURE 1 (1) Whole body vascular cast of adult *X. laevis*. Ventral view. Stereomicroscopic image. Note different size and shape of right (rl), middle (ml) and left lobe (ll) of the liver. (2) Microvascular anatomy of the liver of adult *X. laevis*. Vascular corrosion cast (VCC). Scanning electron micrograph. View at the viscero-pleural surface. Encircled area marks the liver hilus where portal vein (pv) and hepatic artery (ha) approach and the hepatic vein (hv) leaves the liver parenchyma. **Inset** Serrated margin (arrow) of a right hepatic lobe. VCC. Scanning electron micrograph. (3) Right lobe of the liver of adult *X. laevis*. Intraparenchymal course and branching patterns of the hepatic portal vein. Ten branching generations (1–10) of the sub-surface located portal vein are labelled. Superficial sinusoids of the viscero-pleural surface are removed by microdissection. Note the marginal anastomosis (asterisk) between branches of the hepatic vein (hv). VCC. Scanning electron micrograph. Differentiation of portal venules (pv; blue) from hepatic venules (hv; blue/green) was by the presence of hepatic arterioles (ha) which flanked the former, but lacked in the latter. **Inset** Right lobe of liver. Viscero-pleural aspect. VCC. Stereomicroscopic image

interconnected with many neighboring sinusoids forming an ample three-dimensional meshwork (Figure 4-3). Diameters of sinusoids ranged from 15 μm at narrowings to 60 μm at outpouchings. Locally, small "holes" and slit-like openings between individual sinusoids were found (Figure 4-4). Tapering blind-ending vascular structures and close by 4 μm thin sinusoids were rare (Figure 4-4). Sinusoids emptied via their outlet portion

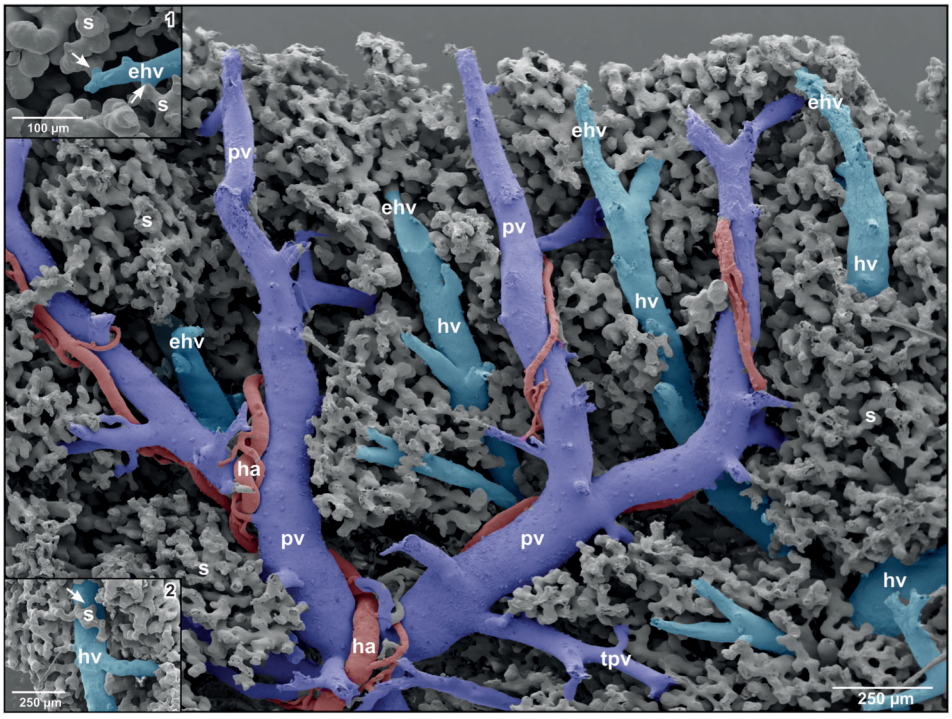

FIGURE 2 Spatial arrangement and relations of hepatic portal vein branches (pv), terminal portal venules (tpv), efferent hepatic venules (ehv), hepatic venules (hv) and hepatic arteries/arterioles (ha). Note that parallel running portal vein branches (pv) and branches of the efferent hepatic veins (ehv) are closely spaced. **Inset 1** Transitions of sinusoids (s) into an efferent hepatic venule (ehv). Note the tube-like outlet portions of sinusoids (s) (arrows). **Inset 2** Sinusoid (s) draining into a larger hepatic venule (hv)(arrow)

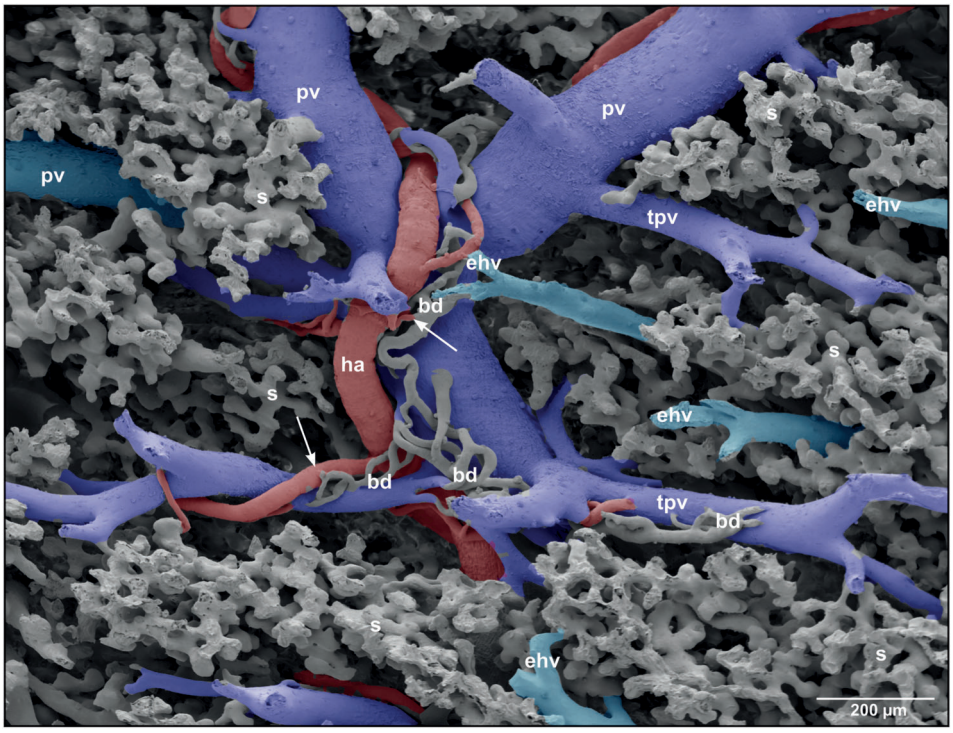

FIGURE 3 Microvascular anatomy of a portal triad consisting of portal vein (pv), hepatic artery (ha) and bile duct (bd). Note the peribiliary plexuses ensheathing fragments of small bile ducts

into differently sized efferent hepatic venules (Figure 2, insets 1 and 2).

Efferent hepatic venules frequently ran parallel to terminal portal venules and approached each other with distances below 100 µm (Figures 2 and 3). Transition distances from terminal portal venules to post-sinusoidal efferent hepatic venules at these sites were rather short (Figure 2). The sinusoidal areas, which drained into an individual efferent hepatic venule, were rather large (Figure 4-3, encircled area). Three to four main hepatic vein branches were found with one large branch running close along the lateral margin of hepatic lobes (Figure 1-3). A veno-venous anastomosis (VVA) was found to connect medial and lateral branches of the hepatic vein

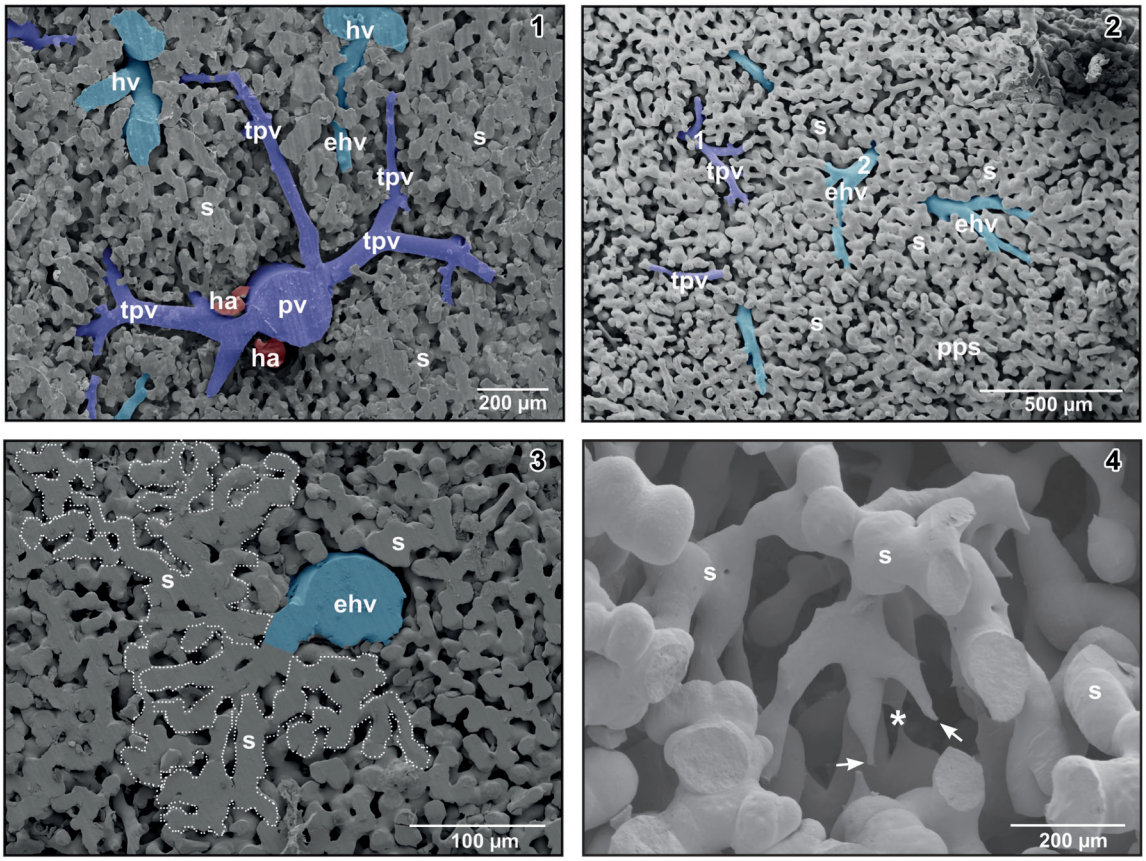

FIGURE 4 (1) Spruce tree-like branching pattern of a portal venule (pv). Detail from a transverse sectioned specimen. Note an efferent hepatic venule (ehv) between terminal portal venules (tpv). (2) Vascular pattern of the parieto-pleural surface of the liver. Note terminal portal venules (tpv, 1) and efferent hepatic venules (ehv, 2). (3) Territory of interconnected sinusoids (encircled area) which drains into an efferent hepatic venule (ehv). (4) Three-dimensional network of sinusoids (s) displaying blind ending tapered vascular structures (arrows) as signs of ongoing sprouting angiogenesis. Note the close by thin sinusoid (asterisk)

(Figure 1-3). Generally, these branches are located dorsal to the main branches of the hepatic portal vein, but occasionally some branches ran also beneath the portal vein branches.

The hepatic artery was a branch of the celiac artery. Approximately at the level of the caudal margins of the liver lobes it bifurcated into a right and a left hepatic artery. Left and right hepatic arteries approached hepatic lobes at the hiluses close aside the hepatic portal vein (Figure 1-2). They showed an average luminal diameter of 0.38–0.46 mm. Before entering the parenchyma, arterial branches ran slightly aside or in close vicinity to the corresponding branches of the hepatic portal vein (Figure 1-2). Intraparenchymal, hepatic arteries flanked the distributing and supplying portions of the portal vein up to terminal portal venules with diameters >100 µm. At this level, they ended by anastomosing with the portal vein (Figure 5-1). The caliber ratios of terminal portal venules vs. flanking hepatic arterioles increased during their joint courses from proximal to distal. Luminal diameter ratios of the portal vein and the accompanying hepatic artery at the hilus were in the range of 2.5:1. Towards distal, ratios increased to 4.5:1 and higher (Figure 5-1). Rarely, two hepatic arterioles flanked a portal venule. Generally, hepatic arteries ran over longer distances parallel to the portal veins; locally they wound around portal veins (Figures 4 and 5).

On their course, hepatic arteries repeatedly branched off arterioles, which emptied into the adjacent portal vein forming arteriolar-portal venular anastomoses (APAs) (Figures 5-1 and -2). At their origin, these branches revealed imprints of intimal cushions (Figure 5-1, inset). At the inlet portions into portal venules, hepatic arterioles sometimes widened trumpet-like (Figure 5-1). Distances between APAs varied. The closest APAs found was a triplet with distances of about 19 µm between inlets (Figure 5-2, inset) followed by distances of about 70 µm (Figure 5-1) and 160 µm (Figure 5-2). Luminal diameters of APAs ranged from 8 to 20 µm.

Hepatic arterioles also anastomosed with sinusoids forming ASAs. They connected directly with wide sinusoids (Figure 5-2) or with straight tubular inlet portions

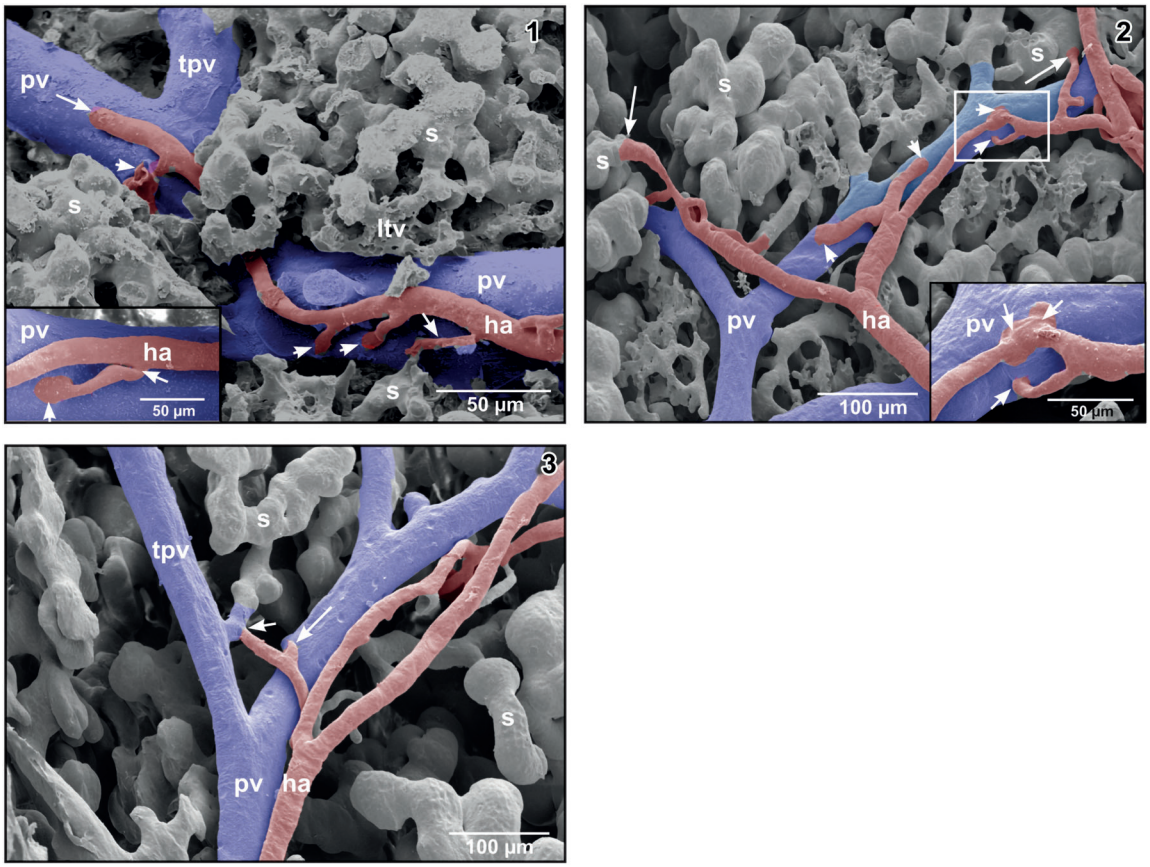

FIGURE 5 (1) Hepatic arteriole (ha) running along a portal venule. Note that the arteriole first gives off a branch to a sinusoid forming an arteriolar-sinusoidal anastomosis (ASA; small arrow), then two branches to the fellow portal venule forming arteriolar-portal (venous) anastomoses (APAs; arrowheads) to finally anastomose with the fellow portal venule (large arrow). **Inset** Short arteriolar-portal anastomosis (APA). Note the widened inlet portion (arrowhead) and the narrowing of the hepatic arteriole at its origin from the parent hepatic arteriole (arrow). (2) Arteriolar-portal (APAs) and ASAs. Note spacing and trumpet-like shape of the arteriolar inlet portions in APAs (arrowheads) and ASAs (arrows). **Inset** Enlargment of the framed area displaying three closely spaced APAs (arrows). (3) Hepatic arteriole joining a tubular inlet portion of a sinusoid (short arrow). The long arrow points at an arteriole that in this angle of view seems to join the portal venule, but does not do so. This was confirmed by changing the tilting angle during SEM work

of sinusoids (Figure 5-3). ASAs were short and were confined to the periportal regions. They were few in number and were widely spaced. Only occasionally two ASAs were found in close neighborhood.

Intraparenchymally, hepatic arterioles gave off short arterioles to the close by small peribiliary vascular plexuses ensheathing small intrahepatic bile ducts (Figure 3). Peribiliary plexuses ascended towards the viscero-pleural liver surface and ran subcapsular (Figure 6-1). They revealed a dense one-layered capillary network fed by hepatic arterioles and drained into adjacent portal venules (Figures 6-1 and -2).

Locally, a rather homogenously looking three-dimensional network of delicate resin structures was found around terminal portal venules and hepatic venules (Figure 7-1). The morphology of this network differed from that of the sinusoids as it consisted of much thinner structures, which formed a honeycomb-like network (Figure 7-1, encircled areas). These networks were fed by hepatic arterioles (Figure 7-2) and drained either into terminal portal venules or into sinusoids (Figure 7-3).

4 | DISCUSSION

Most of what we know about the liver microvascular anatomy originates from studies in mammals and humans. These studies show convincingly that intraparenchymal branches of the portal vein form terminal portal venules, which supply the sinusoids. Sinusoids empty into central hepatic venules located in the center of conical polygonal–shaped liver lobules. Central venules gradually merge and form hepatic venules and

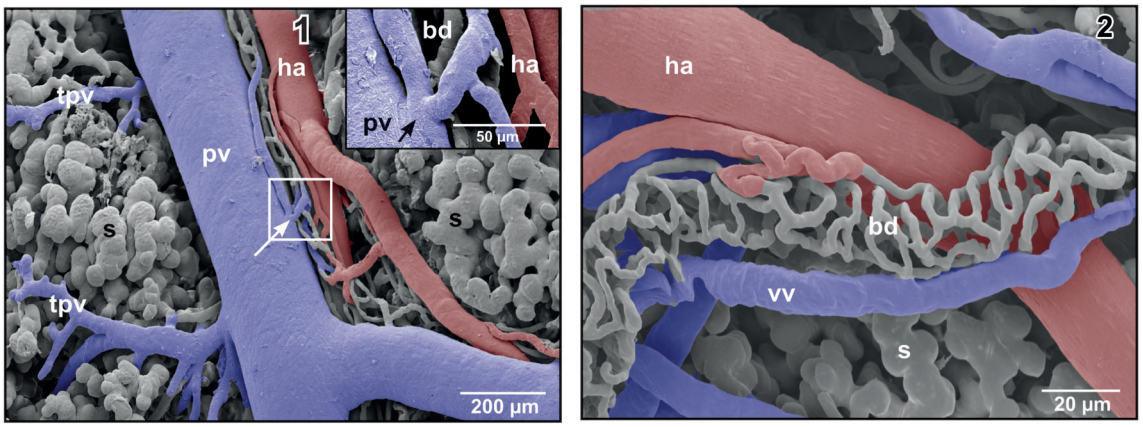

FIGURE 6 (1) Microvascular anatomy of a small subcapsular bile duct (bd) located between portal venule (pv) and hepatic arteriole (ha). The peribiliary vascular plexus drains into the portal venule (arrow). **Inset** Detail (framed area). Note the shallow circular imprint at the inlet site of the efferent peribiliary venules into the portal venule (pv). (2) Microvascular anatomy of a peribiliary vascular plexus of an extraparenchymal bile duct (bd)

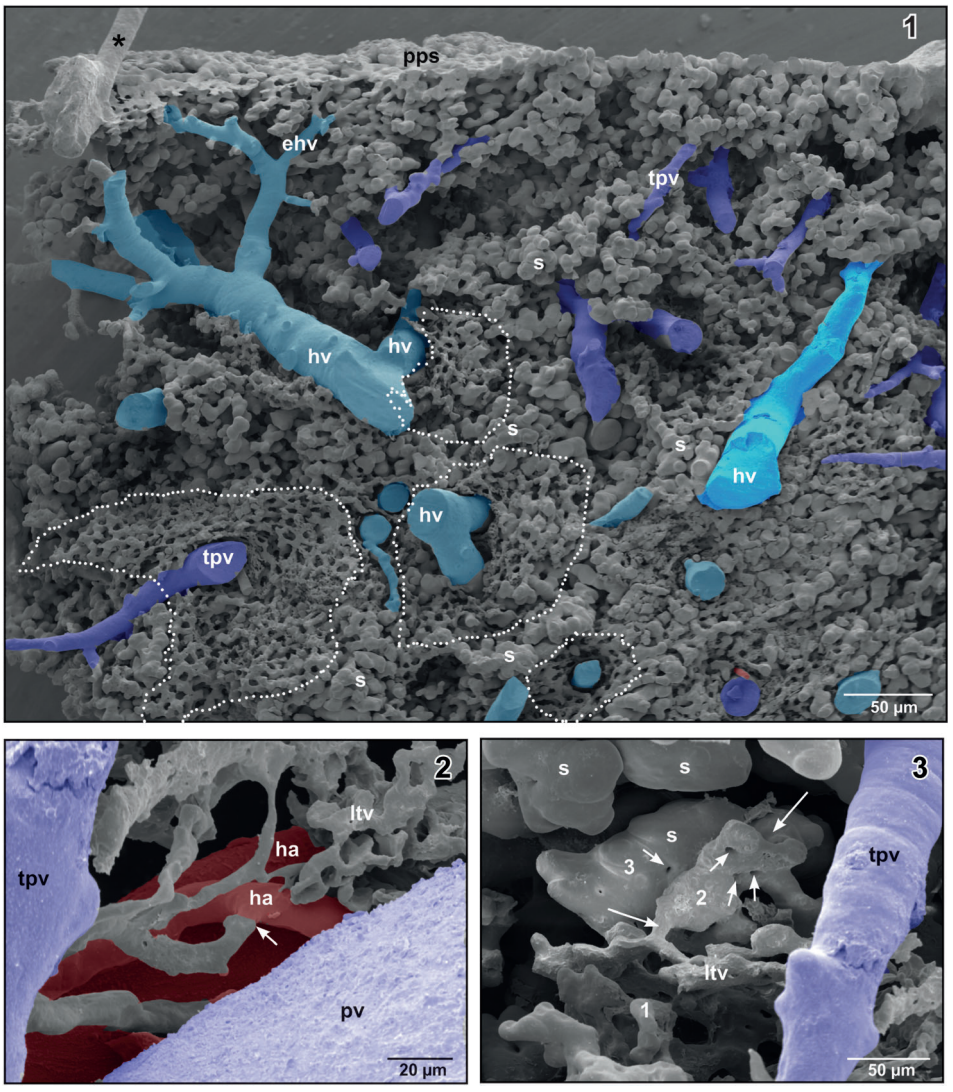

FIGURE 7 (1) Honeycomb-like microvascular meshwork around hepatic venules (hv) and terminal portal venule (tpv) (encircled areas). Asterisk marks "conductive bridge." (2) Arterial supply of the lymphoid tissue vasculature (arrow). (3) Gradual transition (1–3) of the lymphoid tissue vasculature into sinusoids (s) (large arrows). Note the "holes" indicating non-sprouting angiogenesis (small arrows)

veins that finally empty into the posterior (inferior) caval vein. Intraparenchymal branches of the hepatic artery run along the corresponding portal venules. They give off arterioles, which (i) anastomose with sinusoids and form ASAs, (ii) form APAs with terminal portal venules, and (iii) feed the peribiliary capillary plexus of adjacent bile ducts. In some cases, they anastomose with interlobular portal venules (Ohtani & Murakami, 1978).

If we compare our results with those reported on the vascular anatomy of livers of mammals and humans, we find only two differences, namely (i) the lack of central venules and (ii) the lack of efferent peribiliary venules (lobar branches; Ohtani et al., 1982) which in mammalian livers drain into sinusoids (Murakami et al., 1974; Ohtani et al., 1983). The lack of central venules is explained by the non-lobulated structure of the anuran liver. Our finding that the one-layered intrahepatic peribiliary plexuses in *Xenopus* drain via efferent peribiliary venules (prelobular branches; Ohtani, 1981b; Ohtani et al., 1983) into hepatic portal venules (Figures 6-1 and -2) implies that *Xenopus* – other than the monkey (Murakami et al., 1974) – lacks a "peribiliary portal system." Interestingly, Ohtani et al. (1983) reported that in the bullfrog, *Rana catesbeiana,* a peribiliary plexus is present which drains more frequently via lobular branches (efferent peribiliary venules) into hepatic sinusoids then via prelobular branches into portal venules. If these differences in peribiliary plexus drainage of *X. laevis* and *R. catesbeiana* are due to differences in the hepatocyte-sinusoidal structure (HSS) (Akiyoshi & Inoue, 2012) or to methodical differences remains open.

The termination of hepatic arterioles is known to differ between species. In the rat terminal hepatic arterioles as thin as 7 μm in diameter anastomose with branches of terminal portal veins or even with inlet venules of sinusoids, whereas hamster and human livers lack these particular arteriolar-portal (venous) anastomoses (APAs) and terminal hepatic arterioles connect directly to sinusoids (ASAs) (Yamamoto et al., 1985). The liver of monkeys and rabbits lack APAs (Murakami et al., 1974; Ohtani, 1979).

In the rat, Kardon and Kessel (1980) described "arteriolar capillaries" which penetrate deep into the liver lobule to a location equidistant to the central venule and the portal tract. The authors, however, could not find their points of connection to other vessels. Spornitz, Bartuskova, and Morson (2000) reported that in the rat liver even larger branches of the hepatic artery reach far into the liver lobule. In our specimens, we do not find arterioles which penetrate the sinusoidal network that deeply.

In mammals and humans, the sinusoids which are farther away from the portal venules become straighter and more parallel upon joining the central venules (McCuskey, 2008). *Xenopus* lacks such straight parallel running sinusoids.

The APAs and ASAs are generally considered to assist blood flow within sinusoids and to supply oxygen to the liver tissue. Considering their small calibers (8–20 μm) in *Xenopus* their impact on blood flow within terminal portal venules and sinusoids will be low. The fraction of blood delivered by the portal venules to sinusoids, therefore, will be at least as high as in mammals and man (75–80%). Location, dimensions and numbers of APAs and ASAs in the liver of *X. laevis* make them more likely to serve tissue oxygenation than to significantly increase sinusoidal blood flow.

In the present study, we identified branches of the portal vein primarily by the presence of flanking hepatic arteries. Furthermore, branchings of portal veins and venules were more tree-like than in hepatic veins. In cases where no clear identification was possible at a single site the course of the vessel of interest was exposed by removing overlaying vessels under binocular control by fine tipped insect pins until the vessel of interest connected with a clearly defined afferent portal vessel or an efferent hepatic vein (Figure 4-2).

The endothelial cell nuclei imprint patterns found on the surfaces of casts of larger branches of the hepatic portal vein are characteristic for arteries and reflect the high blood flow within portal veins. Similar imprints are present on resin casts of renal portal veins from *X. laevis* (Lametschwandtner & Minnich, 2020).

In the color atlas of *X. laevis* histology, Wiechmann and Wiechmann-Wirsig (2003) document diffuse lymphatic tissue, which locally encircles portal triads (portal vein, hepatic artery, bile duct). In vascular casts of the liver, we find within these areas a three-dimensional meshwork of casted structures that differs from surrounding sinusoids by its delicate honeycomb-like morphology. Based on its location and morphology we consider this meshwork as the vasculature of the diffuse lymphatic tissue, which closely resembles what we previously demonstrated in the periarterial lymphatic sheaths (PALS) of the spleen of *Xenopus* (Lametschwandtner, Radner, & Minnich, 2016). As this vasculature is fed by hepatic arterioles and drains into portal venules and sinusoids, we consider it a fast outlet route for immune cells into liver sinusoids.

At the origins of APAs, ASAs, and terminal portal venules circular imprints or narrowings are present. They reflect sites where single or several vascular smooth muscle cells form sphincters which locally enable to regulate blood flow and tissue oxygenation (Figure 7-2).

Interestingly, the casted liver sinusoids reveal "holes" and "slit-like" imprints of different sizes reflecting sites of intussusceptive microvascular growth (non-sprouting

angiogenesis; Patan, Alvarez, Schittny, & Burri, 1992; Djonov, Baum, & Burri, 2003; Kurz, Burri, & Djonov, 2003; Burri, Hlushchuk, & Djonov, 2004), whereas few tapering blind ending vessels reflecting sprouting angiogenesis. We conclude that non-sprouting angiogenesis (intussusceptive microvascular growth) is the predominating mode of vascular growth and vascular remodeling in the liver of adult *X. laevis*.

ACKNOWLEDGEMENTS

We thank Dr. Heidi Bartel for processing of SEM specimens, Christine Radner, BSc. for assistance in SEM specimen preparation, and Dr. Wolf-Dietrich Krautgartner for excellent technical advice in the SEM facility.

AUTHOR CONTRIBUTIONS

Alois Lametschwandtner: Conceptualization; investigation; methodology; project administration; resources; supervision; writing-original draft; writing-review & editing. **Bernd Minnich:** Conceptualization; investigation; methodology; project administration; resources; supervision; writing-original draft; writing-review & editing. **Udo Spornitz:** Conceptualization; investigation; supervision; writing-original draft; writing-review & editing.

CONFLICT OF INTEREST

The authors declare that they have no competing interests.

ETHICS STATEMENT

The study was approved by the Ethics Committee of the Universität Salzburg, Austria and the Federal Government (BMBWK-66.012/0018-BrGT/2006).

ORCID

Alois Lametschwandtner https://orcid.org/0000-0001-8057-9304

REFERENCES

Adam, H., & Czihak, G. (1964). *Arbeitsmethoden der makroskopischen und mikroskopischen Anatomie*. Stuttgart: G. Fischer Verlag.

Aharinejad, S. H., Böck, P., Lametschwandtner, A., Franz, P., & Firbas, W. (1991). Sphincters in the rat pulmonary veins. Comparison of scanning electron and transmission electron microscopic studies. *Scanning Microscopy*, *5*, 1091–1096.

Aharinejad, S. H., & Lametschwandtner, A. (1992). Microvascular corrosion casting in scanning electron microscopy. In *Techniques and applications*. Wien, New York: Springer-Verlag.

Akiyoshi, H., & Inoue, A. M. (2012). Comparative histological study of hepatic architecture in the three orders amphibian livers. *Comparative Hepatology*, *11*, 2–10.

Bond, A. R., Chih-Wen, N., Hanjoong, J., & Weinberg, P. D. (2010). Intimal cushions and endothelial nuclear elongation around mouse aortic branches and their spatial correspondence with patterns of lipid deposition. *American Journal of Physiology. Heart and Circulatory Physiology*, *298*, H536–H544.

Burri, P. H., Hlushchuk, R., & Djonov, V. (2004). Intussusceptive angiogenesis: Its emergence, its characteristics, and its significance. *Developmental Dynamics*, *231*, 474–488.

Casellas, D., Dupont, M., Jover, B., & Mimran, A. (1982). Scanning electron microscopic study of arterial cushions in rats: A novel application of the corrosion-replication technique. *The Anatomical Record*, *203*, 419–428.

Chen, Y., Yue, X., Zhong, C., & Wang, G. (2016). Functional region annotation of liver CT image based on vascular tree. *BioMed research international*, *2016*, 5428737. https://doi.org/10.1155/2016/5428737.

Debbaut, C., Segers, P., Cornillie, P., Casteleyn, C., Dierick, M., Laleman, W., & Monbaliu, D. (2014). Analyzing the human liver vascular architecture by combining vascular corrosion casting and micro-CT scanning: A feasibility study. *Journal of Anatomy*, *224*, 509–517.

Djonov, V., Baum, O., & Burri, P. H. (2003). Vascular remodeling by intussusceptive angiogenesis. *Cell and Tissue Research*, *314*, 107–117.

Fasel, J. H. D. (2008). Portal venous territories within the human liver: An anatomical reappraisal. *The Anatomical Record*, *291*, 636–642.

Fourman, J., & Moffat, D. B. (1961). The effect of intra-arterial cushions on plasma skimming in small arteries. *The Journal of Physiology*, *158*, 374–380.

Franz, P., Böck, P., Lametschwandtner, A., Breiteneder, H., & Firbas, W. (1990). Sphincter-like structures in corrosion casts. *Scanning*, *12*, 280–289.

Geerts, A., Timmermans, J. P., & Reynaert, H. (2008). Hepatic circulation. *The Anatomical Record*, *291*, 611–613.

Griffin, J. N., Liu, K. J., & Sempou, E. (2020). Editorial: Xenopus models of organogenesis and disease. *Frontiers in Physiology*, *11*, 534.

Häring P. 2004. Die Gefässarchitektur der Leber von *Xenopus laevis*. Inauguraldisseration zur Erlangung der Doktorwürde der Zahnheilkunde, Medizinische Fakultät der Universität Basel. 66.

Kardon, R. H., & Kessel, R. G. (1980). Three-dimensional organization of the hepatic microcirculation in the rodent as observed by scanning electron microscopy of corrosion casts. *Gastroenterology*, *79*, 72–81.

Kurz, H., Burri, P. H., & Djonov, V. G. (2003). Angiogenesis and vascular remodeling by intussusception: From form to function. *News in Physiological Sciences*, *18*, 65–70.

Lametschwandtner, A., & Lametschwandtner, U. (1992). Historical review and technical survey of scanning electron microscopy of vascular casting and scanning electron microscopy. In P. M. Motta, T. Murakami, & H. Fujita (Eds.), *Scanning electron microscopy of vascular casts: Methods and applications* (pp. 1–11). Boston-London: Kluwer Academic Publishers.

Lametschwandtner, A., Lametschwandtner, U., & Weiger, T. (1990). Scanning electron microscopy of vascular corrosion casts. Technique and applications: Up-dated review. *Scanning Microscopy*, *4*, 889–941.

Lametschwandtner, A., & Minnich, B. (2020). Renal microvasculature in the adult pipid frog, *Xenopus laevis*: A scanning electron microscope study of vascular corrosion casts. *Journal of Morphology*, *281*, 725–736.

Lametschwandtner, A., Miodonski, A., & Simonsberger, P. (1980). On the prevention of specimen charging in scanning electron microscopy of vascular corrosion casts by attaching conductive bridges. *Mikroskopie*, *36*, 270–273.

Lametschwandtner, A., Radner, C., & Minnich, B. (2016). Microvascularization of the spleen in larval and adult *Xenopus laevis*: Histomorphology and scanning electron microscopy of vascular corrosion casts. *Journal of Morphology*, *277*, 1559–1569.

McCuskey, R. S. (2000). Morphological mechanisms for regulating blood flow through hepatic sinusoids. *Liver*, *20*, 3–7.

McCuskey, R. S. (2008). The hepatic microvascular system in health and its response to toxicants. *The Anatomical Record*, *291*, 661–671.

Millard, N. (1940). The vascular anatomy of *Xenopus laevis* (Daudin). *Transactions of the Royal Society of South Africa*, *28*, 387–439.

Minnich, B., & Lametschwandtner, A. (2000). Lengths measurements in microvascular corrosion castings - 2D versus 3D morphometry. *Scanning*, *22*(3), 173–177.

Miodonski, A., Hodde, K. C., & Bakker, C. (1976). Rasterelektronenmikroskopie von Plastik-Korrosions-Präparaten: Morphologische Unterschiede zwischen Arterien und Venen. *Beitr Elektr Direktabb Oberfl (BEDO)*, *9*, 435–442.

Motta, P. M., Murakami, T., & Fujita, H. (1992). *Scanning electron microscopy of vascular casts: Methods and applications*. Boston, Dordrecht, London: Kluwer Academic Publishers.

Murakami, T. (1971). Application of the scanning electron microscope to the study of the fine distribution of the blood vessels. *Archivum Histologicum Japonicum*, *32*, 445–454.

Murakami, T., Itoshima, T., & Shimada, Y. (1974). Peribiliary portal system in the monkey liver as evidenced by the injection replica scanning electron microscope method. *Archivum Histologicum Japonicum*, *37*, 245–260.

Ohtani, O. (1979). The peribiliary portal system in the rabbit liver. *Archivum Histologicum Japonicum*, *42*, 153–167.

Ohtani, O. (1981a). Microcirculation studies by the injection replica method. *Biomedical Research*, *2*(Suppl.1), 219–226.

Ohtani, O. (1981b). Microcirculation studies by the injection replica method with special reference to the portal circulations. In D. J. Allen, P. M. Motta, & L. A. J. DiDio (Eds.), *Three-dimensional microanatomy of cell and tissue surfaces* (pp. 51–70). New York: Elsevier North Holland.

Ohtani, O. (1989). Corrosion casts in liver and stomach microcirculation. *Progress in Clinical and Biological Research*, *295*, 317–326.

Ohtani, O., Kikuta, A., Ohtsuka, A., Taguchi, T., & Murakami, T. (1983). Microvasculature as studied by the microvascular corrosion casting/scanning electron microscope method. I. Endocrine and digestive system. *Archivum Histologicum Japonicum*, *46*, 1–42.

Ohtani, O., & Murakami, T. (1978). Peribiliary portal system in the rat liver as studied by the injection replica SEM method. *Scanning electron microscopy*, *1978/II*, 241–244.

Ohtani, O., Murakami, T., & Jones, A. L. (1982). Scanning electron microscopy of replicated liver blood vessels in man and some other animals with special reference to the peribiliary portal system. In P. M. Motta & L. J. A. DiDio (Eds.), *Basic and clinical hepatology* (pp. 85–96). The Hague-Boston-London: Martinus Nijhoff Publishers.

Patan, S., Alvarez, M. J., Schittny, J. C., & Burri, P. H. (1992). Intussusceptive microvascular growth: A common alternative to capillary sprouting. *Archives of Histology and Cytology*, *55*(Suppl), 65–75.

Peeters, G., Debbaut, C., Laleman, W., Monbaliu, D., Vander Elst, I., Detrez, J. R., ... De Vos, W. H. (2017). A multilevel framework to reconstruct anatomical 3D-models of the hepatic vasculature in rat livers. *Journal of Anatomy*, *230*, 471–483.

Porro, L. P., & Richards, C. T. (2017). Digital dissection of the model organism *Xenopus laevis* using contrast-enhanced computed tomography. *Journal of Anatomy*, *231*, 169–191.

Sasse, D., Spornitz, U. M., & Maly, I. P. (1992). Liver architecture. *Enzyme*, *46*, 8–32.

Schraufnagel, D. E., & Patel, K. R. (1990). Sphincters in pulmonary veins. An anatomic study in rats. *The American Review of Respiratory Disease*, *141*, 721–726.

Spornitz, U. (1975a). Studies on the liver of *Xenopus laevis*. I. the ultrastructure of the parenchymal cell. *Anatomy and Embryology*, *146*, 245–264.

Spornitz, U. (1975b). Studies on the liver of *Xenopus laevis*. II. The ultrastructure of the peritoneal cover and the perihepatic layer. *Anatomy and Embryology*, *146*, 265–277.

Spornitz, U. M., Bartuskova, I., & Morson, G. (2000). Microarchitecture of the terminal afferent vessels in the rat liver. A SEM study of vascular corrosion casts. *Microscopy and Microanalysis*, *6*((Suppl 2: Proceedings)), 568–569.

Storch, V., & Welsch, U. (1996). *Kükenthals Leitfaden für das Zoologische Praktikum* (22nd ed.). Stuttgart, Jena, Lübeck, Ulm: Gustav Fischer.

Weiger, T., Lametschwandtner, A., & Stockmayer, P. (1986). Technical parameters of plastics (Mercox CL-2B and various mehtylmethacrylates) used in scanning electron microscopy of vasucular corrosion casts. *Scanning Electron Microscopy*, *1986*, 243–252.

Wiechmann, A., & Wiechmann-Wirsig, C. (2003). *Color atlas of Xenopus laevis histology*. Boston/Dordrecht/London: Kluwer Academic Publishers.

Yamamoto, K., Sherman, I. M., Phillips, J., & Fisher, M. M. (1985). Three-dimensional observations of the hepatic arterial terminations in rat, hamster and human liver by scanning electron microscopy of microvascular casts. *Hepatology*, *5*, 452–456.

How to cite this article: Lametschwandtner, A., Spornitz, U., & Minnich, B. (2022). Microvascular anatomy of the non-lobulated liver of adult *Xenopus laevis*: A scanning electron microscopic study of vascular casts. *The Anatomical Record*, *305* (2), 243–253. https://doi.org/10.1002/ar.24649